

The histone chaperone Spt6 coordinates histone H3K27 demethylation and myogenesis

A Hongjun Wang¹, Hossein Zare¹,
Kambiz Mousavi¹, Chaochen Wang²,
Cara E Moravec³, Howard I Sirotkin³,
Kai Ge², Gustavo Gutierrez-Cruz¹
and Vittorio Sartorelli^{1,*}

¹Laboratory of Muscle Stem Cells and Gene Regulation, National Institute of Arthritis, Musculoskeletal and Skin Diseases, National Institutes of Health, Bethesda, MD, USA, ²Laboratory of Endocrinology and Receptor Biology, National Institute of Diabetes and Digestive and Kidney Diseases, National Institutes of Health, Bethesda, MD, USA and ³Department of Neurobiology and Behavior, Stony Brook University, Stony Brook, NY, USA

Histone chaperones affect chromatin structure and gene expression through interaction with histones and RNA polymerase II (PolII). Here, we report that the histone chaperone Spt6 counteracts H3K27me3, an epigenetic mark deposited by the Polycomb Repressive Complex 2 (PRC2) and associated with transcriptional repression. By regulating proper engagement and function of the H3K27 demethylase KDM6A (UTX), Spt6 effectively promotes H3K27 demethylation, muscle gene expression, and cell differentiation. ChIP-Seq experiments reveal an extensive genome-wide overlap of Spt6, PolII, and KDM6A at transcribed regions that are devoid of H3K27me3. Mammalian cells and zebrafish embryos with reduced Spt6 display increased H3K27me3 and diminished expression of the master regulator MyoD, resulting in myogenic differentiation defects. As a confirmation for an antagonistic relationship between Spt6 and H3K27me3, inhibition of PRC2 permits MyoD re-expression in myogenic cells with reduced Spt6. Our data indicate that, through cooperation with PolII and KDM6A, Spt6 orchestrates removal of H3K27me3, thus controlling developmental gene expression and cell differentiation.

The EMBO Journal (2013) 32, 1075–1086. doi:10.1038/emboj.2013.54; Published online 15 March 2013

Subject Categories: chromatin & transcription; differentiation & death

Keywords: ChIP-Seq; H3K27me3; histone chaperone Spt6; muscle gene expression; RNA-Seq

Introduction

Nucleosomes present a physical barrier to the RNA polymerase II (PolII) transcriptional complex. Biochemical and genetic experiments have identified histone chaperones as critical players of transcriptional elongation (Avvakumov *et al*, 2011).

*Corresponding author. Laboratory of Muscle Stem Cells and Gene Regulation, NIH, NIAMS, 50 South Drive, Room 1351, Bethesda, MD 20892, USA. Tel.: +1 301 435 8145; Fax: +1 301 480 9699; E-mail: sartorev@mail.nih.gov

Received: 7 January 2013; accepted: 13 February 2013; published online: 15 March 2013

FACT and Spt6 facilitate the elongation of PolII complex by interacting with and destabilizing histone dimer-tetramer nucleosomal contacts (Belotserkovskaya and Reinberg, 2004). Additionally, these histone chaperones participate in histone reassembling by collecting and repositioning displaced free histones onto transcribed DNA regions after passage of PolII (Bortvin and Winston, 1996; Belotserkovskaya *et al*, 2003; Saunders *et al*, 2003; Youdell *et al*, 2008). Spt6 enhances transcriptional elongation rate (Kaplan *et al*, 2000; Endoh *et al*, 2004; Ardehali *et al*, 2009) and interacts with elongating serine 2-phosphorylated RNA polymerase II (Ser2P-PolII) (Yoh *et al*, 2007), a property which is also required for Spt6 to promote mRNA processing and nuclear export (Yoh *et al*, 2008). During transcriptional elongation, PolII-associated Spt6 likely encounters, displaces, or modifies nucleosomes bearing repressive epigenetic marks, such as Polycomb Repressive Complex 2 (PRC2)-mediated H3K27me3. Zebrafish Spt6 mutants (*pan^{SBU2}*) display several developmental defects, including loss of segmental expression of the muscle developmental regulator MyoD in somites and disrupted muscle differentiation (Kok *et al*, 2007). Overall, these findings indicate a role of Spt6 in controlling transcription and developmental processes, and prompted us to investigate its contribution to mammalian muscle gene transcription and cell differentiation.

We report that Spt6 is recruited along with PolII at chromatin regions of muscle genes and is required for appropriate muscle gene expression and cell differentiation. Besides its known role in facilitating PolII elongation, we describe an additional mechanism through which Spt6 promotes activation of the myogenic gene program. It entails erasure of the repressive H3K27me3 epigenetic mark through Spt6-mediated chromatin association of the H3K27 demethylase KDM6A (UTX). Cells with reduced Spt6 levels or *pan^{SBU2}* embryos display elevated levels of H3K27me3 and repression of the master regulator of muscle development, MyoD. Furthermore, depletion of H3K27me3 via PRC2 interference in Spt6-siRNA cells reactivates muscle gene expression. Overall, our findings assign an additional regulatory role to Spt6 as modulator of epigenetic modifications involved in controlling gene expression during cell differentiation.

Results

Spt6 is enriched at chromatin regions of actively transcribed genes and is necessary for skeletal muscle cell differentiation

We started exploring the role of Spt6 in muscle gene activation and cell differentiation by first defining its genome-wide distribution by ChIP-Seq in undifferentiated C2C12 skeletal muscle myoblasts (MB) and differentiated myotubes (MT). The Spt6 antibody employed in ChIP-Seq recognizes *bona fide* Spt6 protein as documented by immunoblotting with recombinant Spt6 and Spt6 siRNA experiments

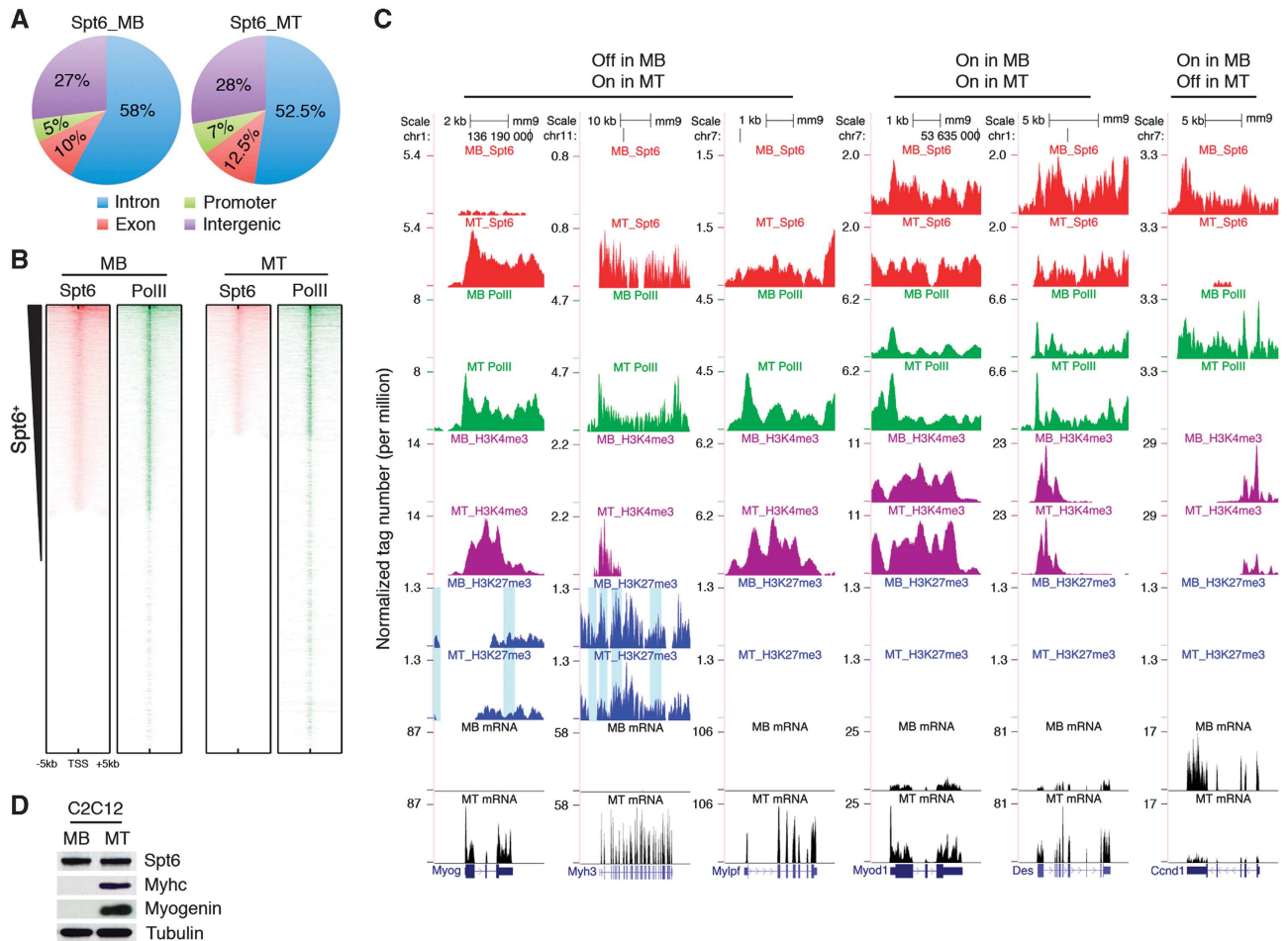


Figure 1 Genome-wide distribution of Spt6 in undifferentiated and differentiated C2C12 skeletal myogenic cells. **(A)** Genome-wide distribution of Spt6 binding in undifferentiated (50% confluent myoblasts, MB) and differentiated (cultured for 48 h in differentiation medium, myotubes MT). The Spt6 ChIP-Seq was performed twice, with two independent biological samples. **(B)** Heat maps representing distribution of Spt6 and PolII binding relative to the gene transcription start site (TSS) in MB and MT. Genes on the heat maps are ordered according to decreasing total level of Spt6 around their TSS. **(C)** Spt6 (red), PolII (green), H3K4me3 (purple), H3K27me3 (blue) occupancies, and RNA-Seq (black) traces for genes preferentially transcribed in MT (*MYOG*, *MYH3*, *MYLP*) in both MB and MT (*MYOD1*, *DES*) or in MB (*CCND1*). Light blue shaded regions at the *MYOG* and *MYH3* indicate genomic regions where H3K27me3 is reduced in MT. **(D)** C2C12 cell extracts immunoblotted with Spt6, myosin heavy chain (Myhc), Myogenin, and tubulin antibodies. Independent biological experiments were done at least three times. Source data for this figure is available on the online supplementary information page.

(Supplementary Figure 1A). With a 5% FDR cutoff, we identified 24 842 and 16 536 Spt6-enriched regions in C2C12 MB and MT, respectively (Supplementary Table 1). In all, 73% of total Spt6 peaks in C2C12 MB and 72% in C2C12 MT were detected within gene bodies and promoters (−1 kb from the transcriptional start site, TSS), while the remaining peaks were located at intergenic regions (Figure 1A). Spt6 was enriched at both TSS and transcription end sites (TES) (Supplementary Figure 1B), a distribution shared with PolII (Kuehner *et al*, 2011). Concurrent analysis of Spt6 and PolII ChIP-Seq for both C2C12 MB and MT (Mousavi *et al*, 2012) revealed that Spt6 positively correlates with PolII occupancy at transcribed genes (Figure 1B; Supplementary Figure 1C and D). Despite being expressed in both MB and MT (Figure 1D), Spt6 was recruited at muscle-specific genes (e.g., *MYOG*, *MYH3*, and *MYLP*) only when these genes were transcribed in MT (Figure 1C). *MYOD1* and *DES*, which were transcribed in both MB and MT, were occupied by Spt6 at both developmental stages, whereas Spt6 occupied *CCND1* only in MB, when the gene is transcribed (Figure 1C). As determined by ChIP-Seq, both *MYOG* and *MYH3* were marked

by H3K27me3. In differentiated MT, H3K27me3 was reduced at selected regions (upstream regulatory regions and gene body of both *MYOG* and *MYH3*) (Figure 1C, shaded regions) (Mousavi *et al*, 2012). Neither Spt6 nor PolII was detected at the neuronal *NEUROGENIN1* locus, which was occupied by H3K27me3 and transcriptionally silent in C2C12 cells (Supplementary Figure 1E). To gain insight into Spt6 function, C2C12 MB cells were transfected with two different sets of Spt6 siRNA duplexes to reduce Spt6 expression. Either set, but not unrelated siRNA, effectively reduced Spt6 protein (Supplementary Figure 1A). When induced to differentiate, C2C12 MB with lowered Spt6 failed to appropriately activate muscle gene expression and differentiate (Figure 2A and B). Similarly, Spt6 knockdown in primary mouse MB negatively affected muscle gene expression and cell differentiation (Figure 2C and D). Conversely, C2C12 cells transduced with Spt6 retroviral vector displayed accelerated differentiation, as shown by precocious expression of MyoG and myosin heavy chains (Myh) (Figure 2E). Overall, these findings indicate that Spt6 accumulates with PolII at transcribed genes and is required for muscle gene expression and cell differentiation.

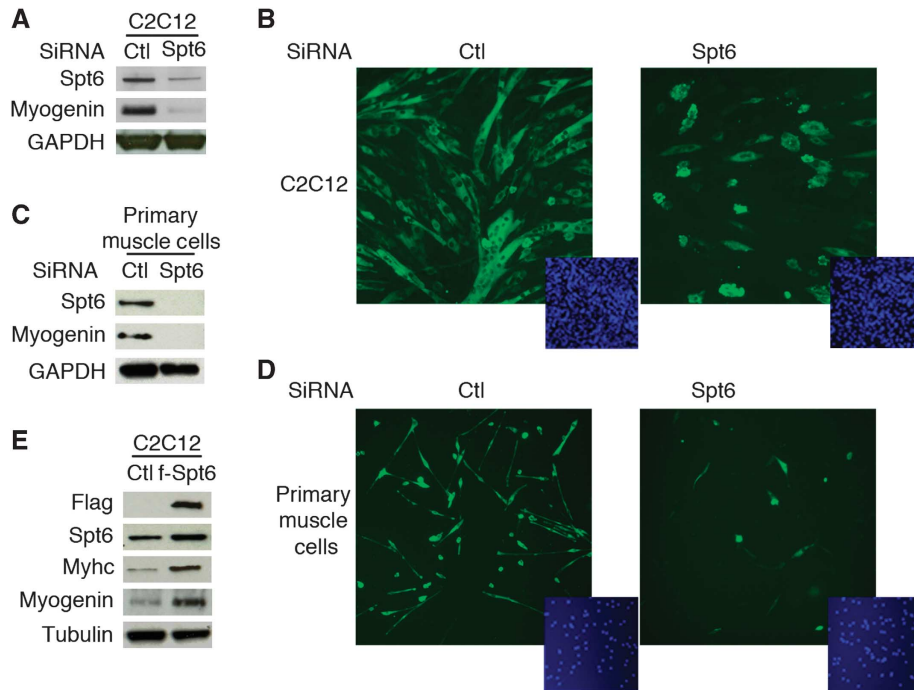


Figure 2 Spt6 regulates muscle gene expression and cell differentiation. (A) C2C12 cells were transfected with control or Spt6 siRNA and extracts were immunoblotted for Spt6, myogenin, and GAPDH antibodies. (B) Immunofluorescence staining of C2C12 cells for Myhc (green) 36 h after transfection with control or Spt6 siRNA. DAPI staining (blue, inset). (C) Primary muscle cells were transfected with control or Spt6 siRNA and extracts were immunoblotted for Spt6, myogenin, and GAPDH antibodies. (D) Immunofluorescence staining of primary muscle cells for Myhc (green) 36 h after transfection with control or Spt6 siRNA. DAPI staining (blue, inset). (E) C2C12 cells transduced with a retrovirus expressing Flag-Spt6 (or control retrovirus) were cultured in differentiation medium for 36 h and the corresponding extracts immunoblotted with Flag, Spt6, Myhc, myogenin, and tubulin antibodies. Independent biological experiments were done at least three times. Source data for this figure is available on the online supplementary information page.

Spt6 negatively regulates H3K27me3 in mammalian cells and zebrafish embryos

To correlate Spt6 and PolII gene occupancies with histone modifications, we performed ChIP-qPCR experiments with antibodies directed against Spt6, PolII, H3K4me3 (a mark of transcriptionally competent promoters), H3K36me3 (transcription elongation mark), H3K27me3 and H3K9me3 (repressive marks) on selected genes in undifferentiated MB and differentiated C2C12 MT. Recruitment of Spt6 and PolII at transcribed genes *MYOG*, *MYH3*, *CKM*, and *SMYD1* correlated with increased PolII, H3K4me3, and H3K36me3 in MT (Figure 3A; Asp *et al*, 2011). H3K27me3 was consistently decreased at every investigated gene in MT, whereas H3K9me3 was reduced only at the *MYOG* and *SMYD1* promoter regions, suggesting distinct and gene-specific functions of these repressive marks (Figure 3A). To investigate whether Spt6 may influence histone modifications and PolII occupancy, C2C12 cells were transfected with control or Spt6 siRNA and ChIP assay performed. In cells transfected with Spt6 siRNA, *MYOG*, *MYH3*, *CKM*, and *SMYD1* genes displayed decreased PolII and H3K36me3 (only at coding regions) (Figure 3B). With the exception of *MYOG*, H3K4me3 was not affected by Spt6 siRNA (Figure 3B). H3K27me3 was significantly increased at every investigated gene and H3K9me3 selectively enriched at the *MYOG* promoter (Figure 3B). Myogenin, Myh3, Ckm, and Smyd1 transcription was reduced by Spt6 siRNA (Figure 3C). These findings, along with the reported chaperone activity of Spt6, prompted us to analyse global levels of histone H3 in control and Spt6-siRNA cells. No obvious differences were detected in either

total or chromatin-bound histone H3 levels (Figure 3D; Supplementary Figure 2A). Surprisingly, H3K27me3 was globally and conspicuously increased (Figure 3D). The effects of Spt6 siRNA on H3K27me3 were specific, as levels of H3K9me3 were not modified (Figure 3D). Even with elevated H3K27me3 levels, total and chromatin-bound Ezh2 protein was reduced (Figure 3D; Supplementary Figure 2B). Spt6 siRNA in a breast cancer cell line or in ESC also caused increased H3K27me3, suggesting that this phenomenon occurs broadly across various mammalian cell types (Figure 3E). A zebrafish mutagenesis screening has identified an Spt6 mutant (*pan*^{SBU2}) with disrupted somitogenesis, defective *MyoD* mRNA expression, and abnormal muscle differentiation (Kok *et al*, 2007). We prepared extracts from sibling wild-type and *pan*^{SBU2} zebrafish embryos and found comparatively reduced *MyoD* protein levels and globally elevated H3K27me3 levels in *pan*^{SBU2} embryos (Figure 3F). Overall, these results indicate that low levels of Spt6 are associated with increased H3K27me3 in several mammalian cell types and in zebrafish embryos.

Spt6 is required for chromatin association of the H3K27 demethylase KDM6A (UTX)

Since increased H3K27me3 in cells with reduced Spt6 could not be attributed to elevated level of Ezh2 (Figure 3D and E; Supplementary Figure 2C), we suspected that Spt6 may modulate H3K27 demethylation processes. KDM6A (UTX) is an H3K27me2/me3-specific demethylase that counteracts PRC2-induced H3K27me3 (Agger *et al*, 2007; Lan *et al*, 2007; Lee *et al*, 2007; Hong *et al*, 2007b) at muscle-specific

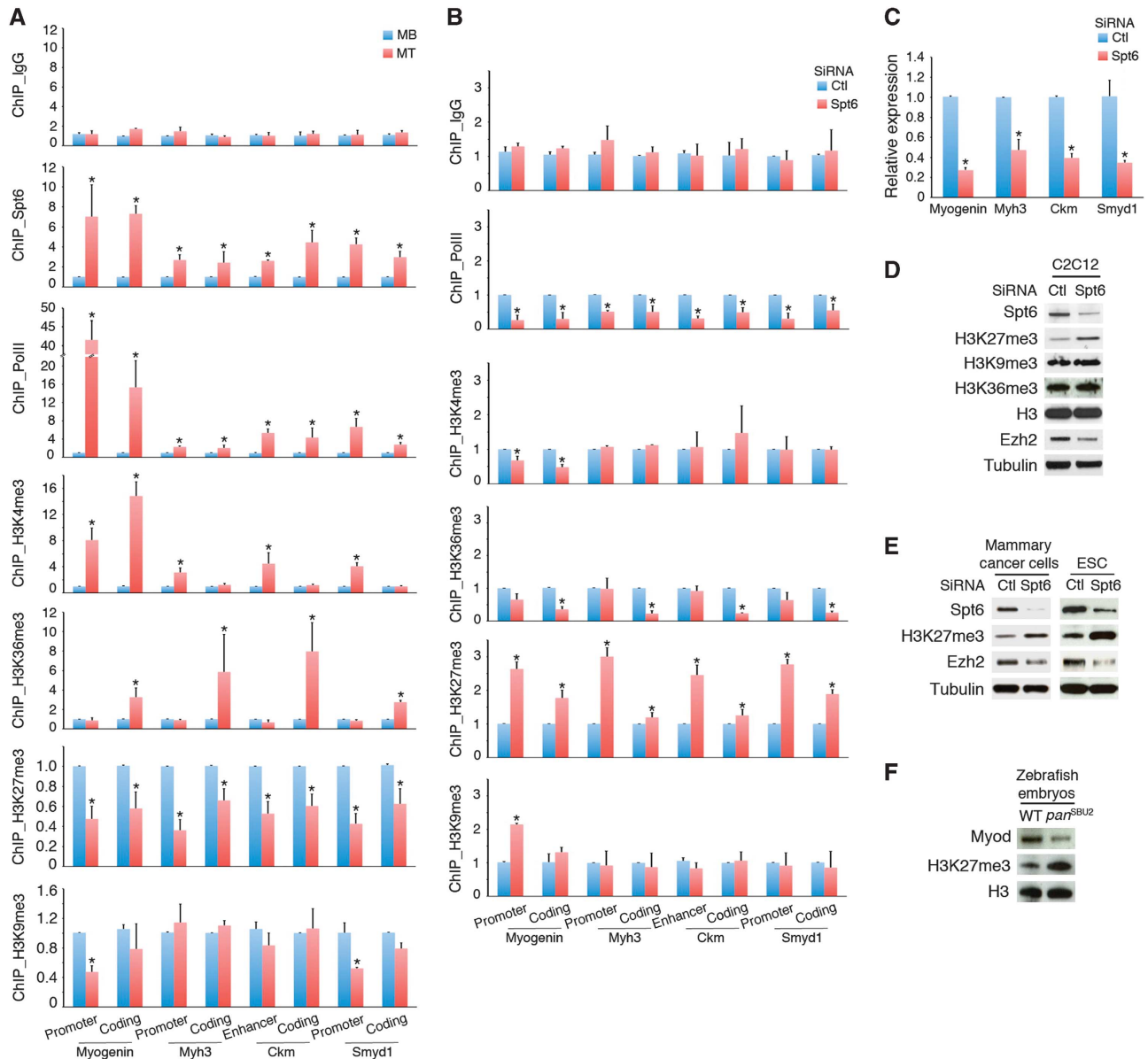


Figure 3 Spt6 influences global and gene-specific H3K27me3 accumulation. (A) ChIP-qPCR with control IgG and antibodies against Spt6, PolII, H3K4m3, H3K36me3, H3K27me3, and H3K9me3 for promoter, enhancer, or coding regions of the indicated genes in MB and MT C2C12 cells. Enrichment values (Y axis) are expressed as fold change normalized to input chromatin. Data are presented as mean \pm s.e.m. ($n = 3$) (*) $P < 0.05$ when compared with C2C12 MB. As the *MYOG* gene is short (1.5 kb), increased H3K4me3 at its coding regions in C2C12 MT likely reflects extension of H3K4me3 signal within the first exon. (B) The antibodies employed in (A) were used for ChIP-qPCR in C2C12 cells transfected with either control or Spt6 siRNA after 36 h culture in differentiation medium. Data are presented as mean \pm s.e.m. ($n = 3$) (*) $P < 0.05$ when compared with cells transfected with control siRNA. (C) RT-qPCR for the indicated transcripts in cells transfected with either control or Spt6 siRNA after 36 h culture in differentiation medium. Data are presented as mean \pm s.e.m. ($n = 3$) (*) $P < 0.05$ when compared with cells transfected with control siRNA. (D) Immunoblot of cell extracts derived from C2C12 cells transfected with control or Spt6 siRNA with antibodies against Spt6, H3K27me3, H3K9me3, H3K36me3, total H3, Ezh2, and tubulin. (E) Cell extracts derived from NK mammary cancer cells and mouse embryonic stem cells (ESC) transfected with either control or Spt6 siRNA were immunoblotted with antibodies against Spt6, H3K27me3, Ezh2, and tubulin. (F) Immunoblot for MyoD and H3K27me3 of extracts from 25 h post fertilization wild-type and *pan^{SBU2}* zebrafish embryos. Independent biological experiments were done at least twice. Source data for this figure is available on the online supplementary information page.

genes (Seenundun *et al*, 2010). Our experiments confirmed KDM6A expression in C2C12 cells and recruitment at both the promoter and coding regions of several genes (Figure 4A and B), coinciding with H3K27 demethylation, H3K4me3 enrichment, PolII engagement, and transcriptional activation (Figure 3A). As shown by experiments in which it was reduced, KDM6A is required for muscle transcriptional activation (Figure 4C). In C2C12 cells transfected with Spt6

siRNA cells, KDM6A chromatin enrichment was reduced (Figure 4E), a phenomenon that was accompanied by increased H3K27me3 (Figure 3B, ChIP_H3K27me3 panel). Total levels of KDM6A were not affected by Spt6-siRNA and, conversely, KDM6A siRNA specifically reduced KDM6A without affecting Spt6 expression (Figure 4D). Thus, Spt6 promotes chromatin association of KDM6A and is required to reduce H3K27me3 at muscle regulatory regions.

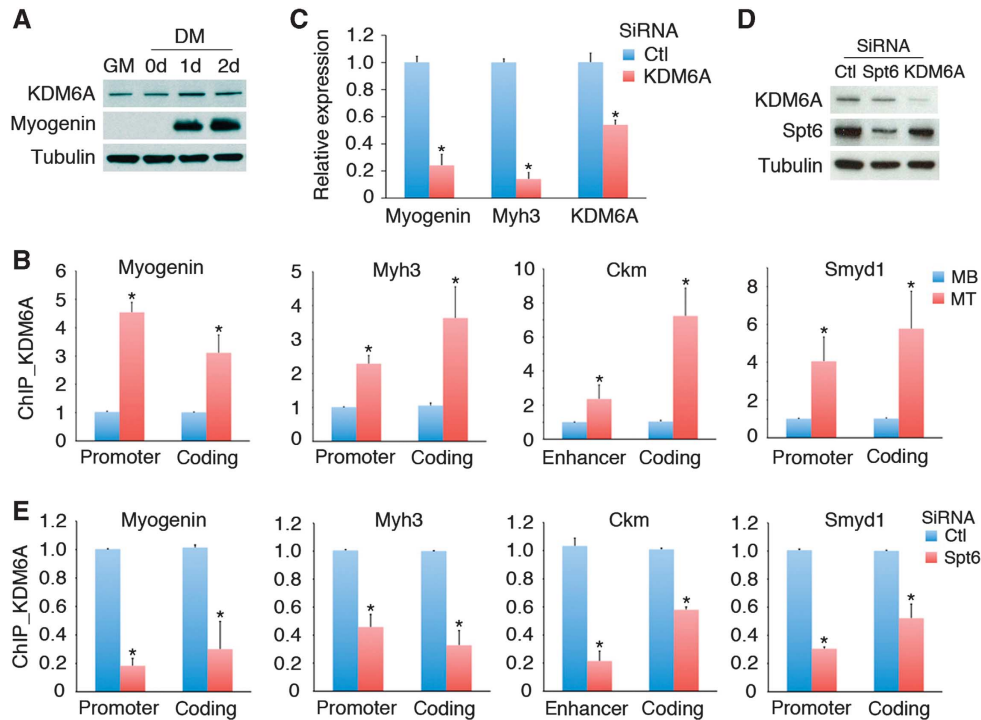


Figure 4 Spt6 is required for chromatin association of the H3K27 demethylase KDM6A (UTX). (A) Immunoblot of cell extracts derived from C2C12 MB and MT with KDM6A, myogenin, and tubulin antibodies. (B) ChIP-qPCR with antibodies against KDM6A at promoter and coding regions of *MYOG*, *MYH3*, *CKM*, and *SMYD1* genes in C2C12 MB and MT. Data are presented as mean \pm s.e.m. Enrichment values (Y axis) are expressed as fold change normalized to input chromatin. Data are presented as mean \pm s.e.m. ($n = 3$) (*) $P < 0.05$ when compared with MB. (C) RT-qPCR for *MyoG*, *Myh3*, and *KDM6A* transcripts in C2C12 cells transfected with control or KDM6A siRNA. Data are presented as mean \pm s.e.m. ($n = 3$) (*) $P < 0.05$ when compared with cells transfected with control siRNA. (D) Immunoblots of KDM6A, Spt6, and tubulin after Spt6 or KDM6A siRNA. (E) ChIP-qPCR with antibodies against KDM6A at *MYOG*, *MYH3*, *CKM*, and *SMYD1* genes in C2C12 cells transfected with control or Spt6 siRNA. Data are presented as mean \pm s.e.m. ($n = 3$) (*) $P < 0.05$ when compared with cells transfected with control siRNA. Source data for this figure is available on the online supplementary information page.

Spt6 and KDM6A are concomitantly recruited at transcribed genes and co-immunoprecipitate

The experiments reported above indicate that Spt6 and KDM6A occupy the same set of muscle regulatory regions. However, Spt6 and KDM6A may independently occupy the same chromatin regions in two different cell subpopulations. To evaluate whether Spt6 and KDM6A concomitantly occupy the same chromatin regions in the same cells, we performed sequential ChIP in which exogenous Flag-tagged Spt6 was first immunoprecipitated with a Flag antibody, the immunoprecipitated material eluted and subjected to a further immunoprecipitation with an antibody directed against endogenous KDM6A. As a control, chromatin from cells transfected with a control ('empty') vector was first immunoprecipitated with Flag antibody followed by immunoprecipitation with the KDM6A antibody. Using ChIP-qPCR, we analysed both the promoter and coding regions of *MYOG*, *MYH3*, *CKM*, and *SMYD1* (Figure 5A). Each region was significantly enriched for KDM6A only in cells expressing Flag-Spt6. Cell transfected with an empty vector displayed no KDM6A enrichment.

The above observations suggested that Spt6 and KDM6A proteins physically interact. To confirm and map the interaction domains, Flag-KDM6A and myc-Spt6 were expressed and co-immunoprecipitated from HEK293 cells. Full-length (a.a. 1–1401) and N-terminus-truncated (a.a. 401–1401) Flag-KDM6A were co-immunoprecipitated with myc-Spt6 (Figure 5B, left panel). The KDM6A N-terminus truncated

region spans a domain with six tetratricopeptide repeats (TPR), an evolutionary conserved motif directly interacting with the acetyltransferase CBP and suggested to mediate the switch from H3K27me3 to H3K27 acetylation (Tie *et al*, 2012). Deletion of the last 143 C-terminal amino acids of KDM6A (a.a. 1–1258) (Figure 5B, right panel) resulted in increased interaction with Spt6, indicating the presence of an interaction inhibitory domain at the C-terminus of KDM6A. Truncation of the JmjC domain (a.a. 1–1095), a motif required for binding to essential cofactors involved in demethylase activity, gave rise to a KDM6A polypeptide which interacted with Spt6 as efficiently as the full-length KDM6A (a.a. 1–1401), whereas the deletion of additional 164 amino acids (a.a. 1–931) substantially diminished KDM6A interaction with Spt6 (Figure 5B, right panel). To map the regions of Spt6 that mediate interaction with KDM6A, we generated several Spt6 deletion mutants (Figure 5C). Two independent regions, one resembling the bacterial Tex-like domain (Johnson *et al*, 2008), the other spanning the RNA binding S1 domain (Bycroft *et al*, 1997) of Spt6 mediated KDM6A interactions. Interestingly, the Src homology 2 (SH2) domain of Spt6, implicated in binding to PolII Ser2 CTD (Yoh *et al*, 2007), was not involved in KDM6A interaction (Figure 5C), leaving open the possibility that PolII, Spt6, and KDM6A may form a trimeric protein complex. Importantly, endogenous Spt6 and KDM6A proteins derived from C2C12 cells also co-immunoprecipitated (Figure 5D). Co-immunoprecipitation experiments conducted with purified baculovirus-produced

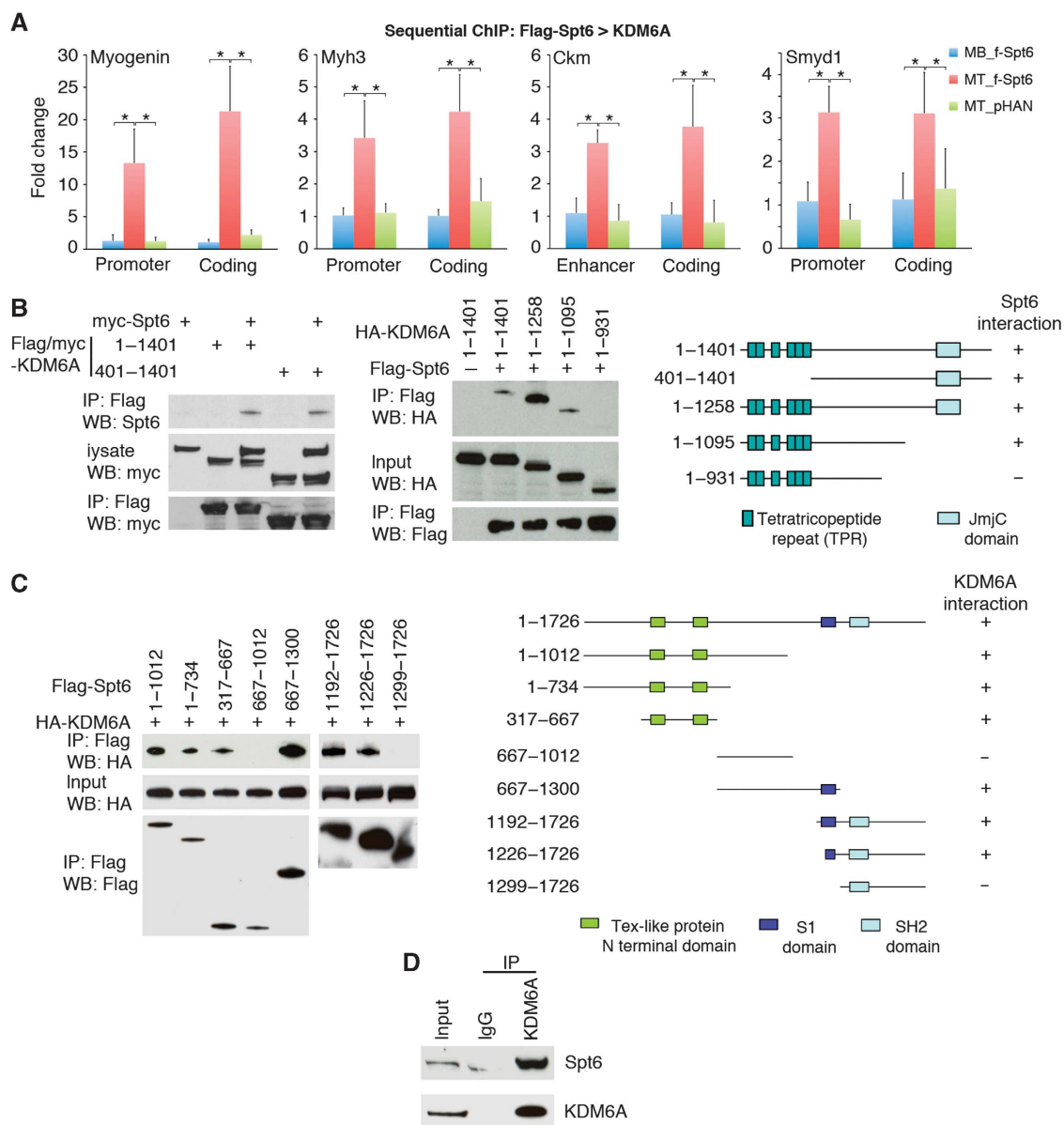


Figure 5 Spt6 and KDM6A co-occupy the same chromatin regions and co-immunoprecipitate. **(A)** Sequential ChIP with antibodies against Flag (flag-Spt6) and KDM6A in C2C12 (MB or MT) cells transduced with a flag-Spt6-expressing retrovirus. The Flag-immunoprecipitated material was re-immunoprecipitated with KDM6A antibodies and qPCR employed to amplify promoter and coding regions of *MYOG*, *MYH3*, *CKM*, and *SMYD1* genes. As control, Flag immunoprecipitation was also performed in C2C12 MT transduced with an empty retrovirus (MT_pHAN). Data are presented as mean \pm s.e.m. ($n = 3$) (*) $P < 0.05$ when compared with C2C12 MB_f-Spt6. **(B)** Mapping interactions of Spt6 and KDM6A. Spt6 and KDM6A constructs were transfected in 293 cells. Extracts from transfected cells were immunoprecipitated with flag resin (M2) and immunoblotted with myc, HA or Spt6 antibodies. **(C)** Flag-Spt6 deletion mutants were coexpressed with HA-KDM6A and immunoprecipitation performed with flag antibodies. Immunoblot performed with HA antibodies. Schematic representation of the immunoprecipitation results (right panels). **(D)** Endogenous Spt6 and KDM6A proteins co-immunoprecipitate. C2C12 extracts were immunoprecipitated with either IgG or anti-KDM6A and immunoblotted for Spt6 or KDM6A antibodies. Source data for this figure is available on the online supplementary information page.

Spt6 and KDM6A failed to detect association of the two proteins (data not shown). Post-translational modifications or adaptor molecules may mediate Spt6-KDM6A interaction.

Genome-wide colocalization of Spt6, PolII, and KDM6A at transcribed genes devoid of H3K27me3

To evaluate the extent of genome-wide overlap of Spt6 and KDM6A binding, we determined the genome-wide distribution of KDM6A by ChIP-Seq in C2C12 MB and MT. KDM6A antibody specificity was documented by immunoblotting

with recombinant KDM6A protein and cell extracts of C2C12 cells with KDM6A siRNA (Supplementary Figure 3A). With a 5% FDR cutoff, ~40 000 and ~21 000 KDM6A-enriched regions were identified in C2C12 MB and MT samples, respectively (Supplementary Table 1). KDM6A ChIP-Seq performed after KDM6A siRNA in C2C12 MB demonstrated genome-wide reduction of KDM6A occupancy, further supporting specificity of the KDM6A antibody (Supplementary Figure 3B and C). Genome-wide distribution of KDM6A in both C2C12 MB and MT closely resembled that of Spt6 (Figure 1) with 68 and 72% of the KDM6A peaks

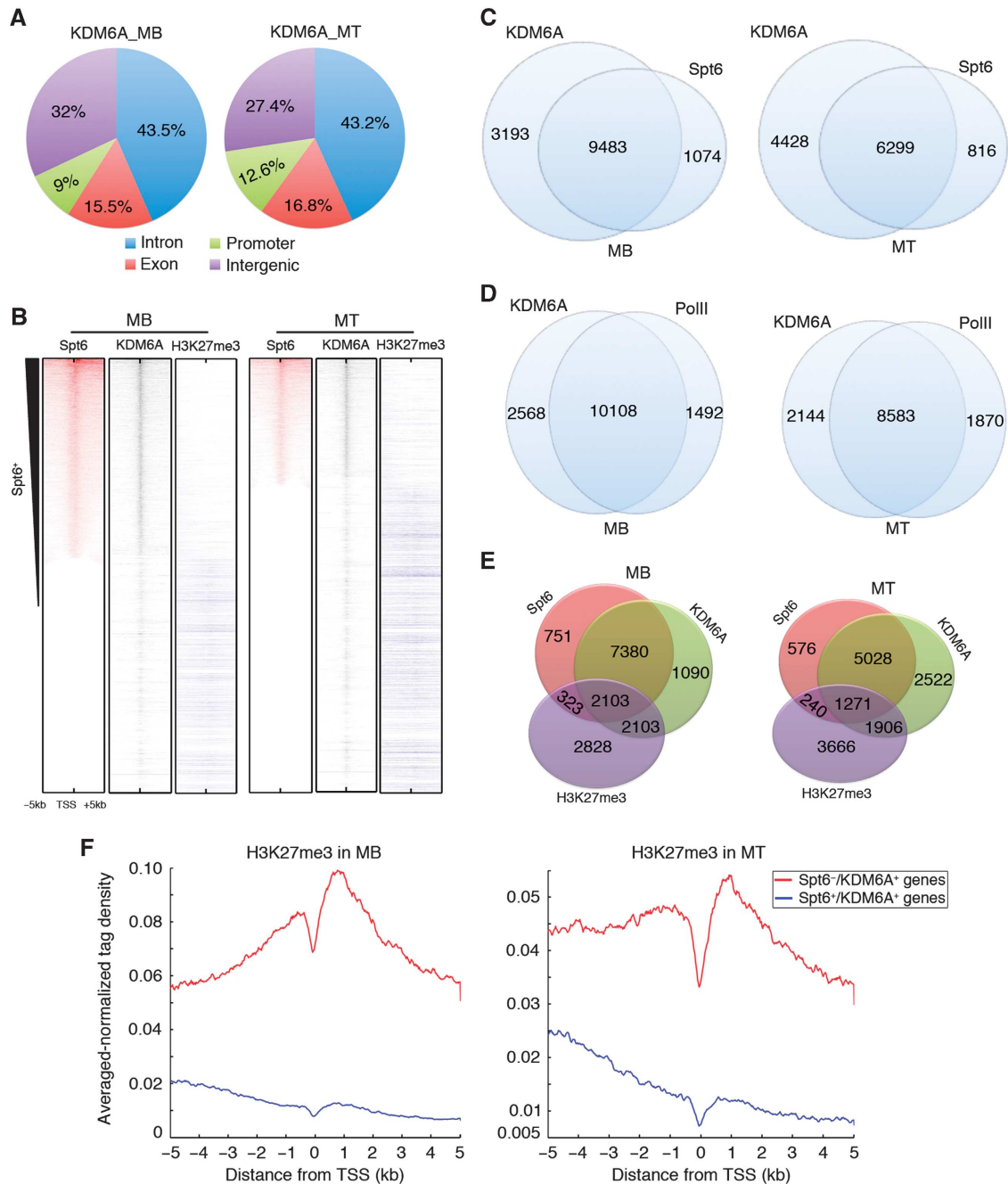


Figure 6 Genome-wide distribution of KDM6A in relation to Spt6, PolII, and H3K27me3. **(A)** Genome-wide distribution of KDM6A binding in MB and MT. **(B)** Heat maps representing distribution of Spt6, KDM6A, and H3K27me3 binding relative to the gene transcription start site (TSS) in MB and MT. Genes on the heat maps are ordered according to decreasing total level of Spt6 around their TSS. **(C–E)** Venn diagrams of genes occupied by KDM6A and Spt6 **(C)**, KDM6A and PolII **(D)** and by Spt6, KDM6A, and H3K27me3 **(E)** in C2C12 MB and MT. **(F)** H3K27me3 enrichment at Spt6⁻/KDM6A⁺ or Spt6⁺/KDM6A⁺ genes in C2C12 MB and MT.

being localized at promoters and gene bodies, and the remaining located at intergenic regions (Figure 6A).

When correlated with ChIP-Seq data sets for Spt6 and PolII, 75% of KDM6A⁺ genes overlapped with Spt6⁺ genes, and 80% of KDM6A⁺ genes overlapped with PolII⁺ genes in C2C12 MB. Similar distributions were observed in C2C12 MT (Figure 6B–D). In addition, KDM6A enrichment at both TSS and TES positively correlated with Spt6 occupancy and was significantly reduced at regions where Spt6 binding was either reduced or not detected (Supplementary Figure 3D),

indicating a dependent binding relation between the two proteins. Spt6- and KDM6A-occupied regions are devoid of H3K27me3 and, conversely, H3K27me3-enriched regions tend to exclude Spt6 and KDM6A binding (Figure 6B).

Intersecting Spt6 and KDM6A with H3K27me3 ChIP-Seq data sets (Mousavi *et al*, 2012) unveiled that 78 and 80% of the Spt6⁺/KDM6A⁺ double-positive genes were devoid of significant H3K27me3 in C2C12 MB and MT, respectively (Figure 6E). To more specifically correlate Spt6 and KDM6A occupancy with H3K27me3, we evaluated H3K27me3

occupancy at two distinct groups of genes. The first group includes genes co-occupied by Spt6 and KDM6A (Spt6⁺/KDM6A⁺). The second group is comprised of a smaller number of genes (~3000), which are occupied by KDM6A but not by appreciable levels of Spt6 (Spt6⁻/KDM6A⁺). This analysis revealed that the average H3K27me3 signal at the Spt6⁻/KDM6A⁺ genes was much higher than that at the Spt6⁺/KDM6A⁺ genes (Figure 6F). Moreover, comparison of the average KDM6A signal at two gene groups displayed a lower KDM6A signal at the Spt6⁻/KDM6A⁺ genes (Supplementary Figure 3D, compare Spt6⁻ with Spt6⁺ traces). Altogether, these analyses indicate that Spt6 binding correlates positively with genome-wide KDM6A recruitment and negatively with H3K27me3 occupancy.

Reducing H3K27me3 rescues the transcriptional defects caused by Spt6 deficiency

Our data are consistent with a model wherein Spt6 mediates KDM6A chromatin association to demethylate H3K27me3 nucleosomes. In this scenario, increased H3K27me3 observed, when Spt6 is experimentally reduced, would be the consequence of the inability of KDM6A to access H3K27me3 nucleosomes and promote their demethylation. A prediction of this model is that the global increase in H3K27me3 observed in Spt6 siRNA cells would not occur in the absence of KDM6A. To test the proposed model, we derived mouse embryonic fibroblasts (MEFs) from E12.5 KDM6A-floxed (KDM6A^{fl/fl}) mouse female embryos (Wang *et al*, 2012). KDM6A^{fl/fl} MEFs were stably infected with a Cre-expressing retrovirus to excise KDM6A (KDM6A^{-/-}) (Figure 7A). As shown for C2C12, breast cancer, and ES cells (Figure 3), Spt6-siRNA increased H3K27me3 also in wild-type MEFs (Figure 7B). Compared to control, KDM6A^{-/-} MEFs had elevated H3K27me3. However, H3K27me3 was not further increased by Spt6-siRNA in KDM6A^{-/-} MEFs, indicating that the effects of Spt6 inactivation on H3K27me3 are mediated by KDM6A (Figure 7B). An additional prediction made by our model is that if transcriptional repression observed in Spt6-siRNA C2C12 cells is the outcome of increased H3K27me3, the reduction in H3K27me3 may reactivate gene expression. To test this prediction, we reduced expression of Ezh2 by siRNA in Spt6-siRNA C2C12 cells. Ezh2-siRNA alone had no significant effect on expression of MyoD (Figure 7C and D). Spt6 siRNA in undifferentiated C2C12 cells resulted in increased H3K27me3 and reduced MyoD expression (Figure 7C and D). Concomitant knockdown of both Ezh2 and Spt6 reduced global and chromatin-bound H3K27me3 compared to Spt6 knockdown alone and reactivated MyoD expression (Figure 7D and E). Consistent with MyoD reactivation, PolII recruitment was re-established in Spt6-Ezh2 double knockdown cells (Figure 7F). Overall, our data indicate that the effects of Spt6-siRNA on H3K27me3 are mediated by KDM6A and that deposition of H3K27me3 allows transcription to resume, even when the levels of Spt6 are suboptimal.

It is noteworthy that mRNA quantification has been performed by correcting for the values of GAPDH mRNA, whose levels are not affected by Spt6 (Yoh *et al*, 2007). Moreover, Spt6 siRNA does affect PolII levels (Yoh *et al*, 2007).

Discussion

The histone chaperone Spt6 interacts with histone H3 and elongating PolII to regulate chromatin dynamics and mRNA biogenesis. Our study reveals that Spt6 plays an additional functional role in promoting and/or stabilizing chromatin interaction of the H3K27 demethylase KDM6A (Figure 7G). Using skeletal muscle cells as a model system, we found that muscle gene expression cannot be properly activated and muscle cells fail to differentiate when Spt6 is experimentally reduced. Under these circumstances, recruitment of PolII at both promoters and gene bodies, and of the H3K27 demethylase KDM6A is hampered at muscle-specific genes, which remain transcriptionally repressed and marked by H3K27me3. Furthermore, expression of muscle master regulator MyoD was repressed and H3K27me3 increased in Spt6 mutant *pan*^{SBU2} zebrafish embryos, confirming the cell culture findings in the animal. Biochemical and ChIP-qPCR experiments indicated that Spt6 and KDM6A co-immunoprecipitate and co-occupy the same muscle regulatory regions. Such biochemical interaction has functional implication in that either downregulation of Spt6 or KDM6A resulted in increased H3K27me3 and silencing of muscle gene expression. Moreover, epistasis experiments demonstrated that, reducing Spt6 in KDM6A^{-/-} cells did not further increase H3K27me3, thus assigning an essential role to KDM6A in mediating increased H3K27me3 in the absence of Spt6.

As Spt6 is devoid of obvious specific DNA-binding modules, its chromatin recruitment may be mediated by specific transcription factors, either directly or through interaction with KDM6A, which is in turn engaged by the transcription factor Six4 at the *MYOG* and *CKM* loci (Seenundun *et al*, 2010). This latter recruitment modality is suggested by the observation that KDM6A is first detected at enhancer and promoter regions and only subsequently spreads to the coding regions of *MYOG* and *CKM*. Moreover, blocking PolII elongation results in increased H3K27me3 at *MYOG* and *CKM* coding regions (Seenundun *et al*, 2010). These findings parallel our results and suggest that protein complexes containing both PolII and Spt6 mediate KDM6A-dependent H3K27 demethylation occurring during the elongation process. In addition to its function at coding regions, KDM6A may be involved in shaping active enhancers by promoting H3K27 demethylation. Suggesting a critical role of KDM6A in establishing enhancer identity, *Drosophila* UTX (dUTX) mutants display a globally reduced H3K4me1 (Herz *et al*, 2010). Indeed, *Drosophila* dUTX is a complex-specific subunit of the *Trr* complex, involved in endowing enhancers with H3K4 monomethylation and H3K27 acetylation (Herz *et al*, 2012). In mammals, KDM6A is found in protein complexes containing MLL3 and MLL4 with H3K4 methyltransferase activity (Cho *et al*, 2007), and cells from MLL3/4 knockout animals display decreased H3K4me1 and H3K27 acetylation and increased H3K27me3 (Herz *et al*, 2012). Thus, it appears that KDM6A might be involved in defining both poised (H3K4m1) (Heintzman *et al*, 2009) and active (H3K4me1/H3K27ac) (Creighton *et al*, 2010; Rada-Iglesias *et al*, 2011) enhancers. Given the intimate relation between KDM6A and Spt6 described here, it will be of interest to determine the role of Spt6 in shaping enhancer landscapes.

Yoh *et al* (2008) have reported that H3K27me3 is globally increased by knockdown of the H3K36me3 methyltransferase

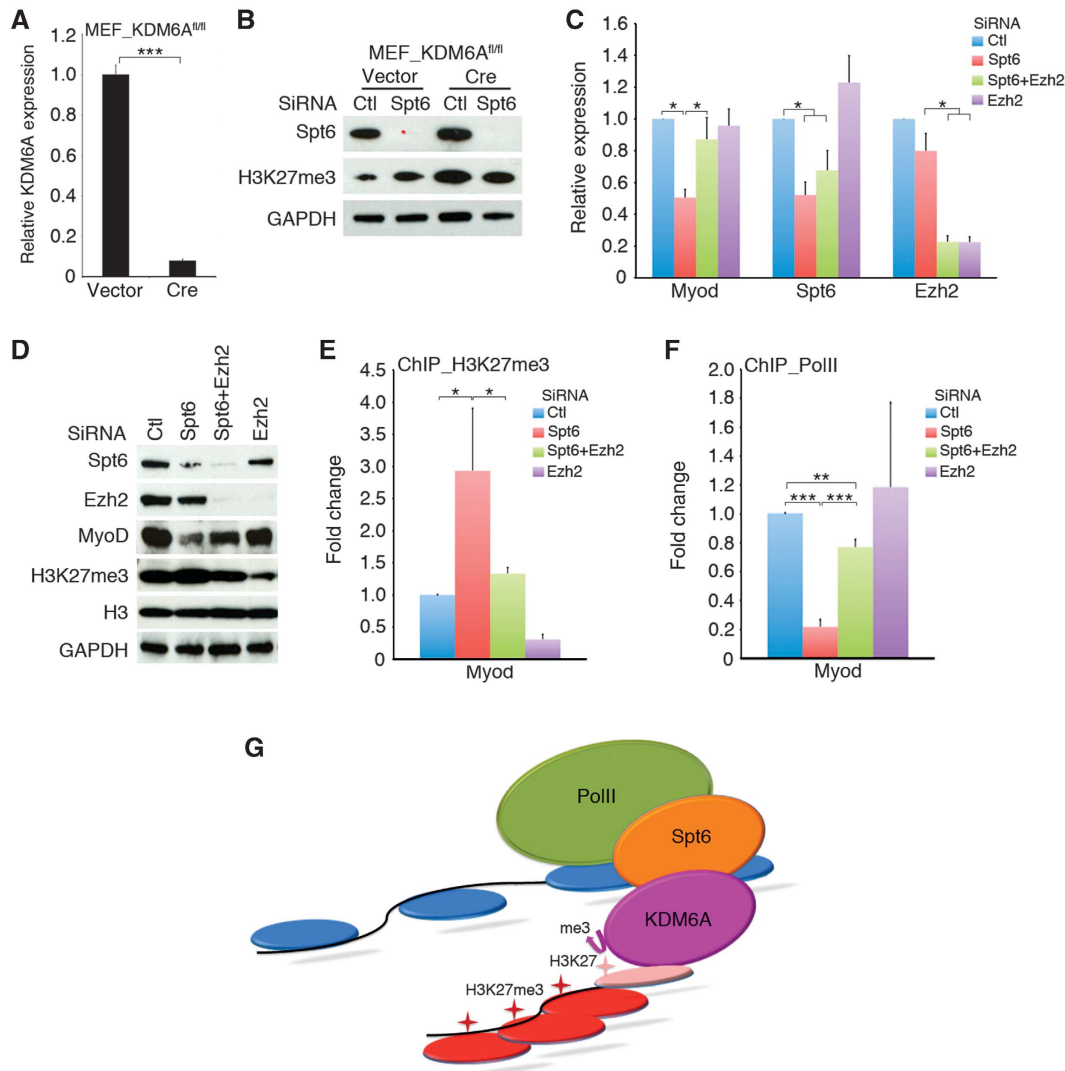


Figure 7 Reducing H3K27me3 rescues the transcriptional defects caused by Spt6 deficiency. (A) RT-qPCR for KDM6A transcripts of KDM6A^{fl/fl} MEFs infected with either control (vector) or a Cre-expressing retrovirus. Data are presented as mean ± s.e.m. (n = 3) (***) P < 0.005. (B) KDM6A^{fl/fl} MEFs infected with control or Cre-expressing retrovirus were transfected with either control or Spt6 siRNA. Cell extracts were immunoblotted with Spt6, H3K27me3, and GAPDH antibodies. (C) RT-qPCR for MyoD, Spt6, and Ezh2 transcripts for C2C12 cells transfected with different combinations of control, Spt6, and Ezh2 siRNAs. Data are presented as mean ± s.e.m. (n = 3) (*) P < 0.05. (D) C2C12 cells were transfected with different combination of control, Spt6 and Ezh2 siRNAs as in (C) and their extracts immunoblotted with Spt6, Ezh2, MyoD, H3K27me3, total histone H3, and GAPDH antibodies. (E) ChIP-qPCR for H3K27me3 gene in C2C12 cells transfected as described in (C). Data are presented as mean ± s.e.m. (n = 3) (*) P < 0.05. (F) ChIP-qPCR for PolII at the MyoD gene in C2C12 cells transfected as described in (C). Data are presented as mean ± s.e.m. (n = 3) (*) P < 0.05; (**) P < 0.01; (***) P < 0.005. (G) Model depicting a hypothetical protein complex consisting of elongating PolII, Spt6, and KDM6A at transitional chromatin regions where KDM6A would promote H3K27 demethylation. Blue nucleosomes represent transcribed regions while red nucleosomes indicate repressed domains. Source data for this figure is available on the online supplementary information page.

HYPB/Setd2, whereas knockdown of Iws1, an Spt6 partner protein specifically increased H3K27me3 of the PABPC1 gene. However, when tested, Iws1 was found not to associate with either KDM6A or B (Yoh *et al*, 2008). Our results suggest that both Setd2 and Iws1 may affect KDM6A recruitment via Spt6. Reducing Spt6 may impair transcription through a combination of reduced PolII recruitment and increased H3K27me3 nucleosomes that may behave as roadblocks, further impeding PolII recruitment and elongation. In agreement with the speculation that H3K27me3 may hinder PolII recruitment and elongation, our findings show that reducing H3K27me3 in Spt6-siRNA cells by interfering with the PRC2 enzymatic subunit Ezh2 allows transcriptional recovery of the muscle master regulator MyoD, indicating

that Spt6 may be dispensable for PolII recruitment and elongation, when H3K27me3 roadblocks are removed (Figure 7F). In a recent study, the H3K27 demethylases KDM6B (JMJD3) and KDM7A (KIAA1718) have been shown to form a protein complex containing the histone chaperones Spt6 and Spt16, the H3K36 methyltransferase SETD2, the chromodomain protein CHD7, and CDC73, a component of the PAF complex (Chen *et al*, 2012). Reduction of either KDM6B or KDM7A decreased Spt6 recruitment at two genes. Thus, Spt6 and H3K27 demethylases KDM6A and KDM6B may be mutually required for effective chromatin recruitment and transcriptional activation. KDM6A controls disparate biological processes, including cardiac developmental program (Lee *et al*, 2012), zebrafish development

(Lan *et al*, 2007), regulation of lifespan in *C. elegans* (Jin *et al*, 2011a) (Maures *et al*, 2011), and retinoblastoma-dependent cell fate (Wang *et al*, 2010). Moreover, KDM6A somatic mutations have been reported in several human tumors (van Haaften *et al*, 2009). Because of the Spt6–KDM6A association, it will be of interest to determine which role Spt6 has in all these processes.

Materials and methods

Cells, plasmids, viral transduction, and transient transfections

C2C12 MB were cultured in DMEM supplemented with 20% FBS (growth media, GM) and induced to differentiate with DMEM supplemented with 2% horse serum, 1 × insulin, transferrin, and selenium (differentiation medium, DM). 293T cells were cultured in DMEM supplemented with 10% FBS. Isolation and culture conditions for mouse primary MB have been described (Caretti *et al*, 2004). Mouse ES cells were cultured in ESGRO-2i Medium (Millipore). *UTX^{fl/fl}* primary MEFs were isolated from E12.5 *UTX^{fl/fl}* female embryos (Wang *et al*, 2012). Retroviral infection of MEFs was done as described (Jin *et al*, 2011b). The mouse mammary cancer cell line NK has been described (Xiao *et al*, 2007). Myc-Spt6 was kindly provided by Dr KA Jones (Yoh *et al*, 2007). Spt6 and deletion mutants were cloned into pCMV-Tag 2 vector (Agilent). The HA-KDM6A vector was kindly provided by Dr K Helin (Agger *et al*, 2007). HA-KDM6A deletion mutants were cloned into pcDNA3.1 vector. Flag/myc-KDM6A and mutant constructs have been described (Hong *et al*, 2007a). Flag-tagged Spt6 was cloned into the pHAN-Puro retroviral vector and transduced in C2C12 cells as described (Caretti *et al*, 2004). Transient transfections were performed using Lipofectamine 2000 (Invitrogen).

RNA interference

Cells were transfected with siRNA against Spt6, KDM6A or Ezh2 with RNAiMAX (Invitrogen) according to manufacturer's protocol. Spt6, KDM6A, and control siRNA oligonucleotides were purchased from Qiagen (Spt6 siRNA #1 SI01438059, Spt6 siRNA #4 SI01438080, and KDM6A siRNA SI01464267, All Star Neg. Control siRNA 1027281). Ezh2 siRNA oligonucleotides have been described (Caretti *et al*, 2004).

Immunofluorescence, immunoblot, and immunoprecipitation

Immunofluorescence was performed as described (Caretti *et al*, 2004). Antibodies used in immunoblots are Spt6 (Novus, NB100-2582), KDM6A (Sigma, HPA000568), MHC and tubulin (Developmental Studies Hybridoma Bank, University of Iowa), GAPDH (Abcam, ab8245), Myogenin (Santa Cruz, sc-576), Ezh2 (Cell Signaling, #5246), Flag (Sigma, F3165), H3K27me3 (Millipore, 07-449), H3K9me3 (Millipore, 07-442), H3K36me3 (Abcam, ab9050), total H3 (Abcam, ab1791 and Cell Signaling, #3638), HA (Santa Cruz, sc-805), and Myc (Millipore, 05-419). For co-IP, 293T cells were cotransfected with plasmids expressing epitope-tagged Spt6 and KDM6A and harvested with lysis buffer (20 mM Tris–HCl (pH 8.0), 10% glycerol, 150 mM NaCl, 5 mM MgCl₂, 0.1% NP-40, protease inhibitors). In all, 1 mg of whole cell lysate was incubated with anti-Flag M2-agarose beads (Sigma). For endogenous Spt6 and KDM6A interactions, C2C12 cells were grown in GM to confluency, nuclear extracts were prepared as described (Wang *et al*, 2000). In all, 500 μg of nuclear extracts were precipitated with normal rabbit IgG (Cell Signaling, #2729) or anti-KDM6A antibody. Bound immunocomplexes were eluted by heating in LDS sample buffer and subjected to Western analysis with anti-Spt6 or anti-KDM6A antibody.

Quantitative RT-PCR

Total RNA was extracted using TRIzol Reagent (Invitrogen). cDNA was synthesized using High Capacity cDNA Reverse Transcription Kit (Applied Biosystems). In all, 2 μl of a 1:10 dilution of the synthesized cDNA was used for quantitative real-time PCR.

RT-qPCR was performed as previously described (Juan *et al*, 2009). Briefly, total RNA was extracted using TRIzol Reagent (Invitrogen). cDNA was synthesized using High Capacity cDNA Reverse Transcription Kit (Applied Biosystems). In all, 2 μl of a 1:10

dilution of the synthesized cDNA was used for quantitative real-time PCR.

ChIP-qPCR, sequential ChIP, and ChIP-Seq

Chromatin immunoprecipitation was performed as previously described (Mousavi *et al*, 2012) using antibodies against Spt6 (Novus, NB100-2582), KDM6A (Sigma, HPA000568), PolII (8WG16, Covance), Ezh2 (Life Technologies, 36-6300), H3K27me3 (Millipore, 07-449 or CS200603), H3K4me3 (Millipore, 07-473), H3K36me3 (Abcam, ab9050), H3K9me3 (Abcam, ab8898), Flag (Sigma, F3165), and IgG (Millipore, PP64B) described in Supplementary data. Real-time PCR was performed with SyberGreen MasterMix (Applied Biosystems). For sequential ChIP, Flag-immunoprecipitated complexes were eluted by incubation for 30 min at 37°C in 25 μl of 10 mM DTT. After centrifugation, the eluted material was diluted 20 times with Re-ChIP buffer as described in Metivier *et al* (2003) and subjected to further immunoprecipitation with KDM6A antibodies. Oligonucleotides employed in ChIP-qPCR are reported in Supplementary Table S2.

ChIP-Seq data analysis

Read alignment. Spt6 and KDM6A ChIP-Seq (36-cycle and 50-cycle single read) were performed on Illumina GAIIX and HiSeq2000 platforms and mapped to the mouse genome (NCBI37/mm9 version) using ELAND algorithm integrated within Illumina parallel sequencing analysis software. Reads aligned, allowing up to two mismatches, to single position in the genome were subsequently used for further analysis. ChIP-Seq for PolII and mRNA-Seq data were obtained and analysed as previously reported (Mousavi *et al*, 2012) and are available at GEO (accession number GSE25549). ChIP-Seq data sets for Spt6 and KDM6A are deposited in GEO (accession number GSE44119).

Peak detection for ChIP-Seq. Read-enriched genomic regions were detected using Spatial clustering approach for the Identification of ChIP-Enriched Regions (SICER) algorithm (Zang *et al*, 2009). This algorithm has been shown to be appropriate to detect broad enriched regions, such as those occupied by PolII and Spt6. To control for false positives, ChIP-Seq data generated from mock DNA immunoprecipitates (input DNA) were used against the sample data in calling enriched regions. Enriched regions were obtained by setting the window size to 200 bp and gap size to 600 bp. Only statistically significant enriched regions based on the FDR of 5% were chosen.

Downstream analyses. All downstream analysis was performed using custom-made programs in Matlab. Gene information, such as TSS and TES, was obtained from UCSC tables (July 2007 NCBI37/mm9 assembly). Heat maps were generated for occupancy profiles around TSS, according to the following: reads in enriched regions were mapped in $-/+5$ kb of TSS using sliding windows of 100 bp with 50 bp overlap. These mapped data were normalized by dividing to the total number of unique mapped tags from corresponding samples, and used to generate heat maps and occupancy profiles of individual ChIPs around TSS and TES. For Supplementary Figure 1C, genes were grouped in five classes. First group are the genes that are not occupied by PolII (PolII⁻ genes). The remaining genes were grouped in four equal sized classes (first, second, third, fourth quartiles) based on their PolII occupancy levels. First quartile genes have the lowest level of PolII occupancy and fourth quartile genes have the highest level. For Supplementary Figure 3D genes were grouped similarly, but Spt6 occupancy levels were used to group the genes. List of genes occupied by each factor was obtained if any peaks were detected in region of -2 kb upstream to $+2$ kb downstream of each gene.

Zebrafish embryos

Adult zebrafish strains and embryos obtained from natural crossing were maintained at 28.5°C. Developmental stages of the embryos were determined according to Kimmel *et al* (1995). Embryos were collected and decorinated with either 1 mg/ml of pronase or by hand. Decorinated embryos were transferred to cold Ringer solution supplemented with 1 mM EDTA and 0.3 mM PMSF. Embryos were passed through a p200 tip to remove the yolks. The deyolked embryos were rinsed twice in fresh Ringer solution containing

EDTA and PMSF. Embryos were then snap frozen in liquid nitrogen after removing the solution and stored at -80°C .

Supplementary data

Supplementary data are available at *The EMBO Journal* Online (<http://www.embojournal.org>).

Acknowledgements

We thank A Derfoul and A Juan (Sartorelli's laboratory) for stimulating discussions. We kindly acknowledge S Yoh and K Jones (Salk Institute, La Jolla, CA) for providing the Spt6 plasmids and K Helin (University of Copenhagen, Denmark) for

the HA-UTX plasmid. This work was supported in part by the Intramural Research Program of the National Institute of Arthritis and Musculoskeletal and Skin Diseases (NIAMS) of the National Institutes of Health (NIH).

Author contributions: AHW and VS conceived the project and AHW performed most of the experiments; KM and GGC performed ChIP-Seq experiments; CEM and CW provided reagents; HZ analysed ChIP-Seq and RNA-Seq data sets; HIS and KG provided input for discussion; AHW, KM, HZ and VS wrote the paper.

Conflict of interest

The authors declare that they have no conflict of interest.

References

- Agger K, Cloos PA, Christensen J, Pasini D, Rose S, Rappasilver J, Issaeva I, Canaani E, Salcini AE, Helin K (2007) UTX and JMJD3 are histone H3K27 demethylases involved in HOX gene regulation and development. *Nature* **449**: 731–734
- Ardehali MB, Yao J, Adelman K, Fuda NJ, Petesch SJ, Webb WW, Lis JT (2009) Spt6 enhances the elongation rate of RNA polymerase II in vivo. *EMBO J* **28**: 1067–1077
- Asp P, Blum R, Vethantham V, Parisi F, Micsinai M, Cheng J, Bowman C, Kluger Y, Dynlacht BD (2011) Genome-wide remodeling of the epigenetic landscape during myogenic differentiation. *Proc Natl Acad Sci USA* **108**: E149–E158
- Avvakumov N, Nourani A, Cote J (2011) Histone chaperones: modulators of chromatin marks. *Mol Cell* **41**: 502–514
- Belotserkovskaya R, Oh S, Bondarenko VA, Orphanides G, Studitsky VM, Reinberg D (2003) FACT facilitates transcription-dependent nucleosome alteration. *Science* **301**: 1090–1093
- Belotserkovskaya R, Reinberg D (2004) Facts about FACT and transcript elongation through chromatin. *Curr Opin Genet Dev* **14**: 139–146
- Bortvin A, Winston F (1996) Evidence that Spt6p controls chromatin structure by a direct interaction with histones. *Science* **272**: 1473–1476
- Bycroft M, Hubbard TJ, Proctor M, Freund SM, Murzin AG (1997) The solution structure of the S1 RNA binding domain: a member of an ancient nucleic acid-binding fold. *Cell* **88**: 235–242
- Caretti G, Di Padova M, Micales B, Lyons GE, Sartorelli V (2004) The Polycomb Ezh2 methyltransferase regulates muscle gene expression and skeletal muscle differentiation. *Genes Dev* **18**: 2627–2638
- Chen S, Ma J, Wu F, Xiong LJ, Ma H, Xu W, Lv R, Li X, Villen J, Gygi SP, Liu XS, Shi Y (2012) The histone H3 Lys 27 demethylase JMJD3 regulates gene expression by impacting transcriptional elongation. *Genes Dev* **26**: 1364–1375
- Cho YW, Hong T, Hong S, Guo H, Yu H, Kim D, Guszczynski T, Dressler GR, Copeland TD, Kalkum M, Ge K (2007) PTIP associates with MLL3- and MLL4-containing histone H3 lysine 4 methyltransferase complex. *J Biol Chem* **282**: 20395–20406
- Creyghton MP, Cheng AW, Welstead GG, Kooistra T, Carey BW, Steine EJ, Hanna J, Lodato MA, Frampton GM, Sharp PA, Boyer LA, Young RA, Jaenisch R (2010) Histone H3K27ac separates active from poised enhancers and predicts developmental state. *Proc Natl Acad Sci USA* **107**: 21931–21936
- Endoh M, Zhu W, Hasegawa J, Watanabe H, Kim DK, Aida M, Inukai N, Narita T, Yamada T, Furuya A, Sato H, Yamaguchi Y, Mandal SS, Reinberg D, Wada T, Handa H (2004) Human Spt6 stimulates transcription elongation by RNA polymerase II in vitro. *Mol Cell Biol* **24**: 3324–3336
- Heintzman ND, Hon GC, Hawkins RD, Kheradpour P, Stark A, Harp LF, Ye Z, Lee LK, Stuart RK, Ching CW, Ching KA, Antosiewicz-Bourget JE, Liu H, Zhang X, Green RD, Lobanenkov VV, Stewart R, Thomson JA, Crawford GE, Kellis M, Ren B (2009) Histone modifications at human enhancers reflect global cell-type-specific gene expression. *Nature* **459**: 108–112
- Herz HM, Madden LD, Chen Z, Bolduc C, Buff E, Gupta R, Davuluri R, Shilatifard A, Hariharan IK, Bergmann A (2010) The H3K27me3 demethylase dUTX is a suppressor of Notch- and Rb-dependent tumors in Drosophila. *Mol Cell Biol* **30**: 2485–2497
- Herz HM, Mohan M, Garruss AS, Liang K, Takahashi YH, Mickey K, Voets O, Verrijzer CP, Shilatifard A (2012) Enhancer-associated H3K4 monomethylation by Trithorax-related, the Drosophila homolog of mammalian Mll3/Mll4. *Genes Dev* **26**: 2604–2620
- Hong S, Cho YW, Yu LR, Yu H, Veenstra TD, Ge K (2007a) Identification of JmjC domain-containing UTX and JMJD3 as histone H3 lysine 27 demethylases. *Proc Natl Acad Sci USA* **104**: 18439–18444
- Hong S, Cho YW, Yu LR, Yu H, Veenstra TD, Ge K (2007b) Identification of JmjC domain-containing UTX and JMJD3 as histone H3 lysine 27 demethylases. *Proc Natl Acad Sci USA* **104**: 18439–18444
- Jin C, Li J, Green CD, Yu X, Tang X, Han D, Xian B, Wang D, Huang X, Cao X, Yan Z, Hou L, Liu J, Shukeir N, Khaitovich P, Chen CD, Zhang H, Jenuwein T, Han JD (2011a) Histone demethylase UTX-1 regulates *C. elegans* life span by targeting the insulin/IGF-1 signaling pathway. *Cell Metab* **14**: 161–172
- Jin Q, Yu LR, Wang L, Zhang Z, Kasper LH, Lee JE, Wang C, Brindle PK, Dent SY, Ge K (2011b) Distinct roles of GCN5/PCAF-mediated H3K9ac and CBP/p300-mediated H3K18/27ac in nuclear receptor transactivation. *EMBO J* **30**: 249–262
- Johnson SJ, Close D, Robinson H, Vallet-Gely I, Dove SL, Hill CP (2008) Crystal structure and RNA binding of the Tex protein from *Pseudomonas aeruginosa*. *J Mol Biol* **377**: 1460–1473
- Juan AH, Kumar RM, Marx JG, Young RA, Sartorelli V (2009) Mir-214-dependent regulation of the polycomb protein Ezh2 in skeletal muscle and embryonic stem cells. *Mol Cell* **36**: 61–74
- Kaplan CD, Morris JR, Wu C, Winston F (2000) Spt5 and spt6 are associated with active transcription and have characteristics of general elongation factors in *D. melanogaster*. *Genes Dev* **14**: 2623–2634
- Kimmel CB, Ballard WW, Kimmel SR, Ullmann B, Schilling TF (1995) Stages of embryonic development of the zebrafish. *Dev Dyn* **203**: 253–310
- Kok FO, Oster E, Mentzer L, Hsieh JC, Henry CA, Sirotkin HI (2007) The role of the SPT6 chromatin remodeling factor in zebrafish embryogenesis. *Dev Biol* **307**: 214–226
- Kuehner JN, Pearson EL, Moore C (2011) Unravelling the means to an end: RNA polymerase II transcription termination. *Nat Rev Mol Cell Biol* **12**: 283–294
- Lan F, Bayliss PE, Rinn JL, Whetstone JR, Wang JK, Chen S, Iwase S, Alpatov R, Issaeva I, Canaani E, Roberts TM, Chang HY, Shi Y (2007) A histone H3 lysine 27 demethylase regulates animal posterior development. *Nature* **449**: 689–694
- Lee MG, Villa R, Trojer P, Norman J, Yan KP, Reinberg D, Di Croce L, Shiekhattar R (2007) Demethylation of H3K27 regulates polycomb recruitment and H2A ubiquitination. *Science* **318**: 447–450
- Lee S, Lee JW, Lee SK (2012) UTX, a histone H3-lysine 27 demethylase, acts as a critical switch to activate the cardiac developmental program. *Dev Cell* **22**: 25–37
- Maures TJ, Greer EL, Hauswirth AG, Brunet A (2011) The H3K27 demethylase UTX-1 regulates *C. elegans* lifespan in a germline-independent, insulin-dependent manner. *Aging Cell* **10**: 980–990
- Metivier R, Penot G, Hubner MR, Reid G, Brand H, Kos M, Gannon F (2003) Estrogen receptor-alpha directs ordered, cyclical, and combinatorial recruitment of cofactors on a natural target promoter. *Cell* **115**: 751–763

- Mousavi K, Zare H, Wang AH, Sartorelli V (2012) Polycomb protein Ezh1 promotes RNA polymerase II elongation. *Mol Cell* **45**: 255–262
- Rada-Iglesias A, Bajpai R, Swigut T, Brugmann SA, Flynn RA, Wysocka J (2011) A unique chromatin signature uncovers early developmental enhancers in humans. *Nature* **470**: 279–283
- Saunders A, Werner J, Andrusis ED, Nakayama T, Hirose S, Reinberg D, Lis JT (2003) Tracking FACT and the RNA polymerase II elongation complex through chromatin in vivo. *Science* **301**: 1094–1096
- Seenundun S, Rampalli S, Liu QC, Aziz A, Palii C, Hong S, Blais A, Brand M, Ge K, Dilworth FJ (2010) UTX mediates demethylation of H3K27me3 at muscle-specific genes during myogenesis. *EMBO J* **29**: 1401–1411
- Tie F, Banerjee R, Conrad PA, Scacheri PC, Harte PJ (2012) Histone demethylase UTX and chromatin remodeler BRM bind directly to CBP and modulate acetylation of histone H3 Lysine 27. *Mol Cell Biol* **32**: 2323–2334
- van Haaften G, Dalgliesh GL, Davies H, Chen L, Bignell G, Greenman C, Edkins S, Hardy C, O’Meara S, Teague J, Butler A, Hinton J, Latimer C, Andrews J, Barthorpe S, Beare D, Buck G, Campbell PJ, Cole J, Forbes S *et al*. Somatic mutations of the histone H3K27 demethylase gene UTX in human cancer. *Nat Genet* **41**: 521–523
- Wang AH, Krullak MJ, Wu J, Bertos NR, Vezmar M, Posner BI, Bazett-Jones DP, Yang XJ (2000) Regulation of histone deacetylase 4 by binding of 14-3-3 proteins. *Mol Cell Biol* **20**: 6904–6912
- Wang C, Lee JE, Cho YW, Xiao Y, Jin Q, Liu C, Ge K (2012) UTX regulates mesoderm differentiation of embryonic stem cells independent of H3K27 demethylase activity. *Proc Natl Acad Sci USA* **109**: 15324–15329
- Wang JK, Tsai MC, Poulin G, Adler AS, Chen S, Liu H, Shi Y, Chang HY (2010) The histone demethylase UTX enables RB-dependent cell fate control. *Genes Dev* **24**: 327–332
- Xiao C, Sharp JA, Kawahara M, Davalos AR, Difilippantonio MJ, Hu Y, Li W, Cao L, Buetow K, Ried T, Chadwick BP, Deng CX, Panning B (2007) The XIST noncoding RNA functions independently of BRCA1 in X inactivation. *Cell* **128**: 977–989
- Yoh SM, Cho H, Pickle L, Evans RM, Jones KA (2007) The Spt6 SH2 domain binds Ser2-P RNAPII to direct Iws1-dependent mRNA splicing and export. *Genes Dev* **21**: 160–174
- Yoh SM, Lucas JS, Jones KA (2008) The Iws1:Spt6:CTD complex controls cotranscriptional mRNA biosynthesis and HYPB/Setd2-mediated histone H3K36 methylation. *Genes Dev* **22**: 3422–3434
- Youdell ML, Kizer KO, Kisseleva-Romanova E, Fuchs SM, Duro E, Strahl BD, Mellor J (2008) Roles for Ctk1 and Spt6 in regulating the different methylation states of histone H3 lysine 36. *Mol Cell Biol* **28**: 4915–4926
- Zang C, Schones DE, Zeng C, Cui K, Zhao K, Peng W (2009) A clustering approach for identification of enriched domains from histone modification ChIP-Seq data. *Bioinformatics* **25**: 1952–1958